THE ASTROPHYSICAL JOURNAL, 297:702–709, 1985 October 15

HIGHLY SUPERSONIC BIPOLAR MASS EJECTION FROM A RED GIANT OH/IR SOURCE: OH 0739−14

MARTIN COHEN
Radio Astronomy Laboratory, University of California, Berkeley, and NASA/Ames Research Center

MICHAEL A. DOPITA
Mount Stromlo and Siding Spring Observatories, Research School of Physical Sciences, Australian National University

RICHARD D. SCHWARTZ
University of Missouri, St. Louis

AND

ALEXANDER G. G. M. TIELENS
Space Science Laboratory, University of California, Berkeley
Received 1985 January 18; accepted 1985 April 5

ABSTRACT

From long-slit spectrophotometry of the bipolar nebula associated with the unusual OH source, OH 0739−14, we are able to show the presence of a blue companion to the M9 III central star and have discovered a Herbig-Haro–like knot beyond each nebular lobe. From differential colors of the lobes and from radial velocities of these knots we demonstrate that the system inclines its northern lobe toward us. We also show that the nebulous knots are shocks being driven into an extensive circumstellar envelope and that this material is very overabundant in nitrogen, suggesting that it is matter lost from a star of mass $>3\ M_{\odot}$. A model of biconical ejection from a central binary is consistent with the OH observations, and we speculate on the possible relation of OH 0739−14 to the symbiotic stars and to bipolar planetary nebulae.

Subject headings: nebulae: reflection — shock waves — stars: binaries — stars: mass loss

I. INTRODUCTION

OH 0739−14, also known in terms of its galactic coordinates as OH 231.8+4.2, is an OH source showing extraordinarily large (~ 100 km s^{-1}) internal motions (Turner 1971). This is associated with an infrared source (Wynn-Williams, Becklin, and Neugebauer 1974) which, at short wavelengths, extends over some $5'' \times 10''$ (Allen *et al.* 1980). In the optical, it is identified with a very red bipolar reflection nebula having lobes aligned roughly north-south (Cohen and Frogel 1977). This reflects the light of a centrally embedded M9 III star (Cohen 1981).

The southern lobe is brighter than the northern one, and such asymmetry is usually interpreted in terms of obscuration of the fainter lobe by an asymmetric circumstellar disk.

The association of OH/IR source, bipolar nebula, and evolved variable red giant star very strongly suggests that here we see the immediate precursor of a planetary nebula: a star caught in a short-lived axisymmetric mass-loss phase during its asymptotic giant branch (AGB) evolution. In this case, the bipolar morphology is reminiscent of the class of highly luminous type I planetary nebulae defined by Greig (1971) and Peimbert (1978), of which NGC 6302 is a good example. If this connection is valid, OH 0739−14 is a key object in understanding the late evolution of the more massive stars that can give rise to planetary nebulae ($\sim$3–5 $M_{\odot}$) and the processes that drive the high mass-loss rates that appear to be required at this phase (Wood and Cahn 1977; Renzini and Voli 1981; Renzini 1981*a*, *b*).

The dynamics of this object in the OH emission have been investigated by Morris and Bowers (1980) and Morris, Bowers, and Turner (1982; hereafter MBT). They demonstrated that maser emission occurs well above and below the inferred equatorial plane and is blueshifted in and around the northern lobe and redshifted in the other lobe. At intermediate velocities a complete ring of emission is seen. MBT attempted to model this in terms of an expanding thick disk, and they inferred that, in this model, the brighter southern reflection lobe would lie closer to Earth.

In this paper we present the results of long-slit spectrophotometry along the axis of the nebula. We show, for the first time, that the faint northern lobe is also a reflection nebula of the central star(s). In both northern and southern lobes we have discovered a blue continuum which may be associated with a companion star. We also demonstrate highly supersonic mass ejection by the discovery of faint Herbig-Haro–like shock-excited emission knots beyond each lobe. From the radial velocities of these knots and the color ratios of the lobes we show that the northern lobe is in fact the closest to Earth, and show how this can be reconciled with the OH data in an overall model of the source geometry.

II. THE OBSERVATIONS

On 1984 April 3 we obtained long-slit spectra using the Royal Greenwich Observatory (RGO) spectrograph of the Anglo-Australian 3.9 m telescope at Siding Spring Observatory. The detector was the image photon counting system (IPCS; Bokesenberg 1972). Using the 25 cm camera of the RGO spectrograph, we obtained a resolution element of 2″.3 in the (spatial) and 2″.6 (spectral) directions. The slit length was 115″ long (50 pixels), and, using a 250 line grating, we obtained 10 Å resolution over a usable wavelength coverage of 3500–7500 Å. The data included observations of the Oke (1974) white dwarf standards and Baldwin and Stone (1984) stars as secondary standards. The data were flat-fielded by dividing

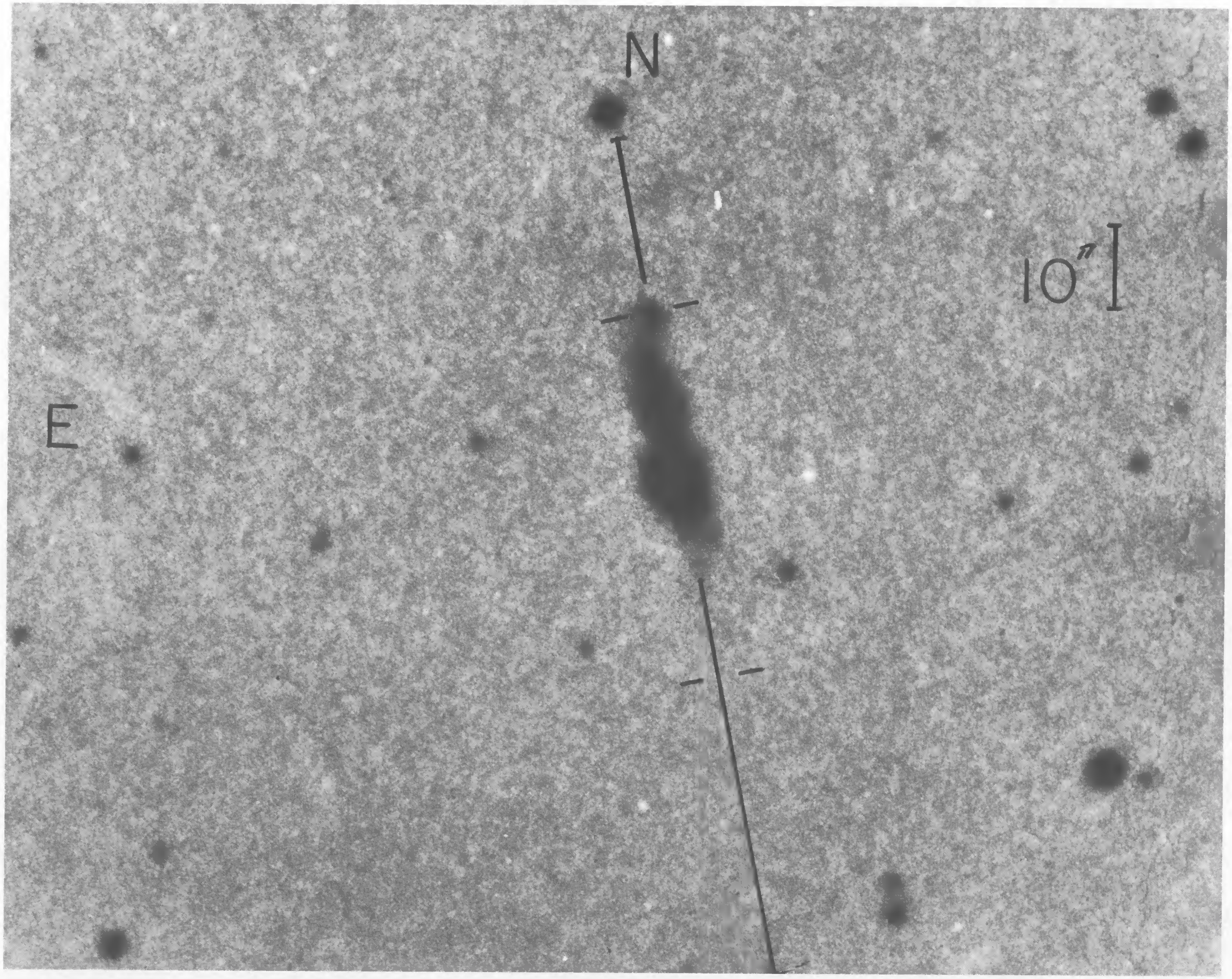

FIG. 1.—Slit position superposed on a near-infrared photograph of OH 0739 − 14, kindly supplied by Judy Cohen. Newly discovered HH objects are indicated by tick marks and are faintly visible just beyond each apex of the reflection lobes.

them by a (normalized) observation of a continuum source lamp, wavelength linearized; following this operation they were *flux calibrated* using mean extinction coefficients of the observing site; they were sky subtracted and finally extracted, all using the PANDORA software package.

Figure 1 illustrates the location and orientation of the slit with respect to the nebulosity.

III. THE NEW EMISSION KNOTS

We have discovered faint wisps of nebulosity associated with both lobes and lying exactly on the long axis of the nebula (Fig. 1). The nebula associated with the southern lobe is $\sim 11''$ long and centered $32''$ south of the equatorial axis of the reflection nebulae. A similar somewhat brighter knot, some $9''$ long, is found $13''$ north of the center of the reflection nebulae. Unfortunately this knot is confused with a star near its brightest point (Fig. 1) which therefore could not be subtracted out. However, the IPCS data show nebular emission over three spatial increments, whereas the star spectrum was confined to one only. We are therefore confident that the star is a field object.

The spectra of these two knots (Fig. 2) are identical to those

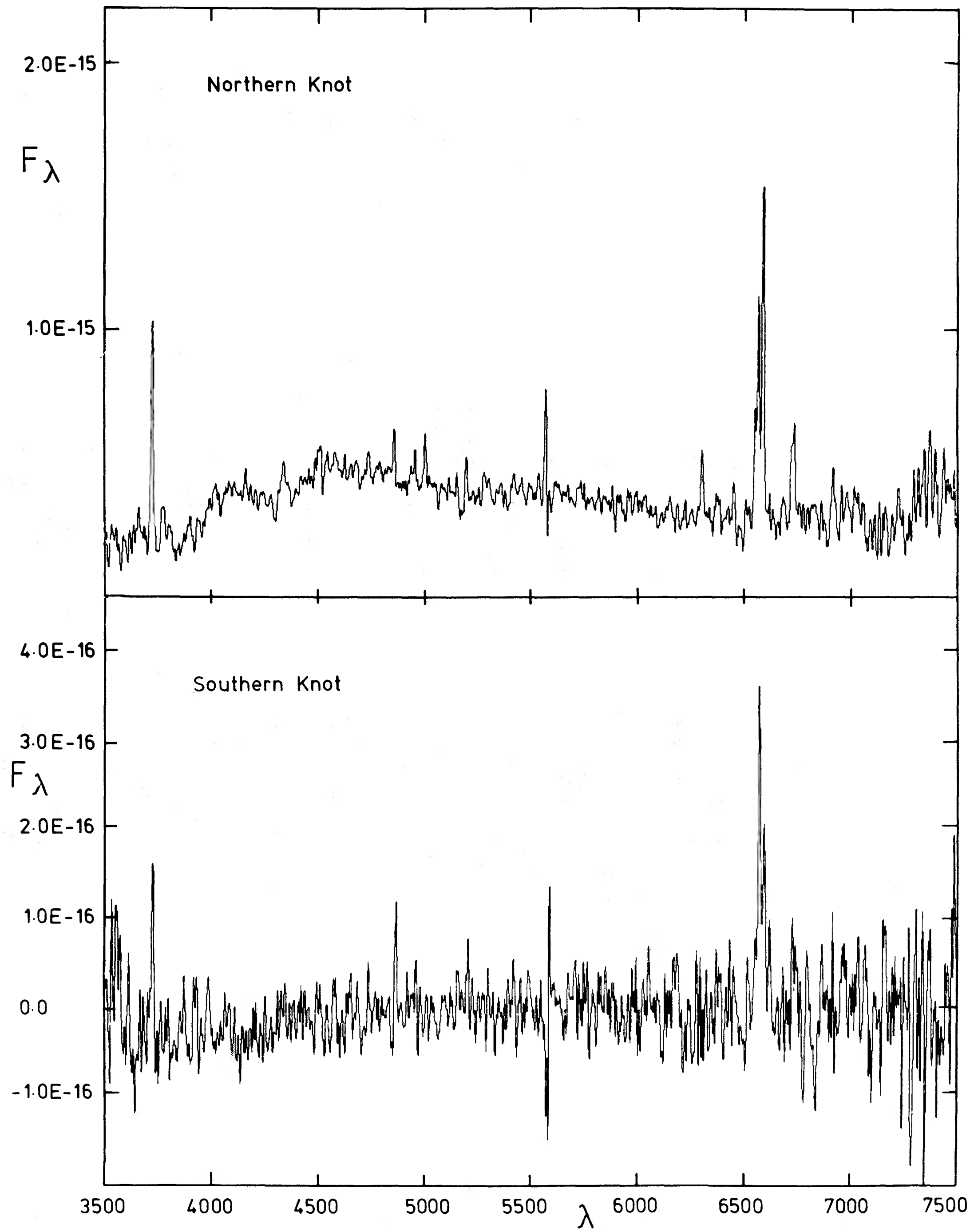

FIG. 2.—Newly discovered Herbig-Haro–like emission knots associated with the northern (*upper*) and southern (*lower*) reflection lobes. Spectrum of the northern knot is confused with that of a field star.

generally associated with Herbig-Haro objects, with strong forbidden lines of low excitation such as [O II], [O I], [S II], [N II], [N I], and [Fe II]. Hitherto such emission spectra have only been seen in association with very young stars, frequently T Tauri stars (Cohen and Schwartz 1979; Cohen 1982; Dopita, Schwartz, and Evans 1982), and it is now generally accepted that such spectra are the result of shock waves (Schwartz 1975; Dopita 1978; Raymond 1979; Dopita, Binette, and Schwartz 1982).

The greater intensity of the [O III], [N II], and [O II] lines in the northern knot shows this to have a higher shock velocity, and the large [S II] $\lambda 6731/\lambda 6717$ ratio indicates a substantial preshock density. We have modeled these spectra using the code MAPPINGS (Dopita *et al.* 1984) in an attempt to reproduce the observed line intensities. In an effort to minimize the number of free variables, we have proceeded iteratively by fixing the elemental abundance ratios at solar and using self-consistent preionization conditions (e.g., Shull and McKee 1979) until the ratios [O III]/[O II], [N II]/[N I], and the [S II] ratio $\lambda 6731/\lambda 6717$ were matched by our shock velocity (V_s) and preshock density (n_1). The absolute abundances of nitrogen and oxygen were then allowed to vary to match the absolute strengths of the nitrogen and oxygen lines with respect to the Balmer lines. The observed and intrinsic line intensities in the knots and the result of the model fits are shown in Table 1. We find for the northern knot preshock density and shock velocities of 250 cm^{-3} and 88 km s^{-1}, respectively; for the southern knot the corresponding figures are 30 cm^{-3} and 65 km s^{-1}.

The overabundance of nitrogen in these models is both large and significant, and we take this as evidence of the presence of CN–processed material in the outflowing material presumably originally ejected from the central red giant star. In stellar evolution theory, such CN–processed material can result from hot-bottom burning and convective dredgeup (Becker and Iben 1979; Renzini and Voli 1981), although a stellar mass of at least 3 $M_\odot$ is required for this to be effective.

Another dimension to the expansion of the knots is added by the direct determination of their radial velocities. Based upon the seven best-determined lines in the S knot and the 11 lines of highest signal-to-noise ratio in the N knot we discover that the S knot has a 146 ± 42 km s^{-1} redshift with respect to the N knot. Using the observed wavelengths of the night-sky lines as a check on the absolute wavelength scale, we find heliocentric radial velocities of $+108 \pm 29$ km s^{-1} for the S knot and -38 ± 13 km s^{-1} for the N knot. These figures can be converted to LSR by subtracting 17.8 km s^{-1}. We are confident, as has been demonstrated by Bowers and Morris (1984), that mass ejection rather than inflow characterizes this source. This result therefore demonstrates that the northern lobe is the closer of the two. This result is interesting in view of the fact that the intrinsic Balmer decrement shows the northern emission knot to be considerably more obscured than the southern one [A_v(N-knot) ≈ 1.5 mag; A_v(S-knot) ≈ 0.7 mag]. This difference is presumably associated with the difference in density inferred from the shock diagnostics of Table 1.

IV. THE REFLECTION NEBULOSITY

In Figure 3 we show the spectra of the two nebular lobes. The deeply mutilated appearance of the red spectra result from the presence of TiO band heads. Based on the strengths of these (e.g., Cohen 1981) and both the presence and strength of the VO band head at 7400 Å, we classify the star seen in reflection in both lobes as M9. Previously only the southern lobe had definitely been identified as being a reflection nebula (Cohen 1981). We cannot, on the basis of these spectra, provide independent luminosity criteria, and so we follow Cohen (1981), who classified the central star as M9 III on the basis of the strength of the $\lambda 7699$ resonance line of K I. A giant, rather than supergiant, identification was also proposed by MBT on the basis of their OH/IR observations.

Below about 5500 Å, the spectra of both lobes show a faint, but real, blue continuum which maximizes around 4200 Å. The quality of the data is too poor to permit classification, but neither spectrum is consistent with the cool stellar spectrum seen in the red. In the absence of either appreciable radio continuum, emission, or any indications of ionized material near the central star, this is the first observational indication that this star may in fact be a binary and therefore is possibly related to the symbiotic stars (Allen 1984).

TABLE 1

OBSERVED INTRINSIC AND MODEL-FITTED LINE I INTENSITIES IN KNOTS

λ (Å)	Ion	Observed Fluxes[a] N Knot	Observed Fluxes[a] S Knot	Intrinsic Fluxes[b] N Knot	Intrinsic Fluxes[b] S Knot	Models[c] N Knot	Models[c] S Knot
3727.........	[O II]	1.65(−14)	3.14(−15)	899	205	664	364
4861.........	Hβ	3.01(−15)	1.89(−15)	100	100	100	100
4959.........	[O III]	1.70(−15)	...	54	...	48	...
5007.........	[O III]	3.40(−15)	<2.40(−16)	107	...	139	...
5158.........	[Fe II]	1.52(−15)	8.14(−16)	45	41	...	...
5200.........	[N I]	3.02(−15)	1.13(−15)	88	57	25	105
6300.........	[O I]	5.28(−15)	<2.50(−16)[d]	110	...	66	60
6548.........	[N II]	6.59(−15)	1.01(−15)	126	42	143	56
6563.........	Hα	1.57(−14)	7.21(−15)	300	300	296	314
6584.........	[N II]	2.35(−14)	3.57(−15)	448	148	421	165
6717.........	[S II]	3.27(−15)	1.17(−15)	61	48	53	89
6731.........	[S II]	6.47(−15)	1.30(−15)	119	53	106	101

[a] Flux units: ergs cm^{-2} s^{-1}.

[b] Corrected to Hβ = 100.0 for mean reddening of knots, assuming an intrinsic flux ratio of Hα/Hβ of 3.0.

[c] Self-consistent preionization shock models. Solar abundances used except for nitrogen (3.5×10^{-4} by number with respect to hydrogen) and for oxygen (9.4×10^{-4} by number with respect to hydrogen).
Shock parameters: N knot: $V = 88$ km s^{-1}; $n_1 = 250$ cm^{-3}; S knot: $V = 65$ km s^{-1}; $n_1 = 30$ cm^{-3}.

[d] Line lost in night sky [O I].

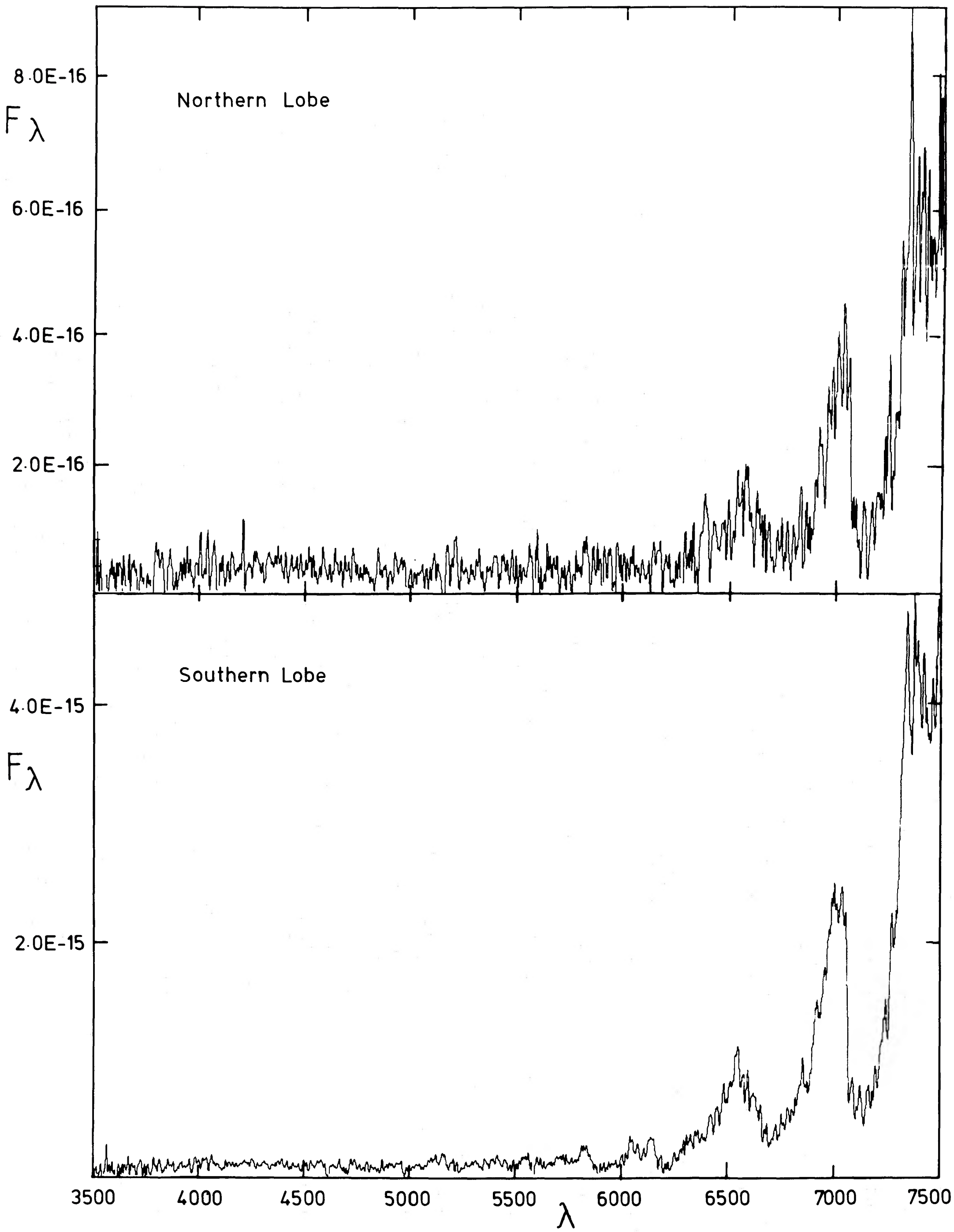

FIG. 3.—Spectra of the northern (*upper*) and southern (*lower*) reflection lobes. Note the M-type spectrum in the red and the faint but real detection of both lobes in the blue.

The differential color of the two lobes is particularly interesting. The intensity ratio of the northern to the southern lobe decreases with wavelength (i.e., the northern lobe is bluest; see Table 2). Such a color difference might be explained in terms of extinction in a circumstellar disk which preferentially obscures the southern lobe. However, the southern lobe is in fact the brighter of the two. Furthermore, the reddening in the line of sight to the HH knots has been shown to be greater for the northern knot than for the southern one. Infrared observations of the scattered light in the lobes produce a similar result (Tielens, Werner, and Capps 1985). To reconcile these three observational facts (bluer color, lower brightness, and greater external reddening in the northern lobe) requires a model which allows for extinction near the star, the extinction and scattering geometry in the lobe, and the distribution of dust external to the lobe.

Some progress can be made if we bear in mind that the velocity and density measurements on the HH knots described

TABLE 2

FLUX RATIOS OF NORTH/SOUTH LOBES

Wavelength (Å)	Flux Ratio[a]	Error (±)
3750.........	0.44	0.05
4250.........	0.40	0.03
4750.........	0.40	0.03
5250.........	0.33	0.05
5750.........	0.33	0.06
6250.........	0.24	0.03
6750.........	0.16	0.01
7250.........	0.15	0.01

[a] Average in a 500 Å wide bin.

in the previous section prove that the northern lobe is tilted toward us and has higher density. With this geometry, the light of the northern lobe will be dominated by forward-scattering, whereas back-scattering will prevail in the southern lobe. Provided the scattering results on large dielectric grains, the ratio of forward-scattering to back-scattering amplitudes is a very strongly decreasing function of wavelength (e.g., Isobe 1975). For example, for silicate grains 0.16 μm in diameter, this ratio falls from 37 to 1.65 between 3000 and 7000 Å. The increasing absorption efficiency of the dust at shorter wavelengths and multiple scattering effects may prevent the full effect of this change in scattering ratio being seen in the color ratio of the lobes, but nevertheless we would expect the bluest lobe, the northern, to be the closest to Earth.

The higher density inferred for the northern lobe is consistent with the higher extinction observed to the HH knot in this lobe. The lower surface brightness of the northern knot could therefore result from two effects: first, this higher external extinction and, second, multiple scattering in the lobe itself which would produce a lower effective albedo of the dust.

V. DISCUSSION

The preceding discussion has shown that the optical nebulosity associated with OH 0739−14 is reflecting the light of an M9 giant and another object that gives a blue continuum. The existence of high-velocity mass motions in both lobes is demonstrated by the Herbig-Haro–like nebulous knots. The location of these knots, exactly on the axis of bipolarity and near the tips of each lobe of the nebula, implies that they must be formed by one of two shock processes.

The first possible process is that the Herbig-Haro–like shocks are intrinsic to an outflowing jet. Such shocks occur in a jet before turbulence generated at the boundary can disrupt the flow and may be either biconical or conical with transverse Mach disks (such as are frequently seen in rocket exhausts). These shocks may either be stationary in the flow or move outward. However, in general, the shock velocity indicated by the excitation will not match the knot velocity derived from the radial velocity and proper motion.

The second possible process is that the shocks are formed at the work surface of a stellar wind focused by interaction with a preexisting circumstellar disk in which there is a steep density gradient in the polar directions (Canto 1980; Canto and Rodriguez 1981; Konigl 1982). In this case, if the radiative shock is the one moving into the circumstellar material, the knot velocity and the shock velocity will match. However, if the radiative shock is generated in the stellar wind, this will not be true.

In the case of OH 0739−14, it is possible to test between these models, using the known inclination of the axis of the nebula derived from near-infrared polarimetric studies (Tielens, Werner, and Capps 1985). These observations showed that the nebula is inclined by 47° to the plane of the sky. Using the data of Bowers and Morris (1984), this then implies a distance of 1.2 kpc. From the radial velocity data, correcting for inclination effects, the combined expansion of the knots along the major axis should be 200 ± 61 km s^{-1}. From our shock diagnostics of Table 2, we find the sum of the shock velocities is 154 ± 15 km s^{-1}. These numbers are sufficiently similar to exclude the possibility that the shocks are formed intrinsically in the outflowing material, and therefore must be the result of a shock pushed into preejected matter by the overpressure of the recently ejected material. In this case, this pressure can be calculated from the shock parameters and amounts to 4.4×10^{-8} dynes cm^{-2} in the N knot and 3.2×10^{-9} cm^{-2} in the S knot. If the distance of OH 0739−14 is 1.2 kpc then a mass loss given by

$$\dot{M} = 25 \times 10^{-7} \Omega_{10} v_{100}{}^{-1}\ M_{\odot}\ \mathrm{yr}^{-1}$$

is required to drive the N knot, where Ω_{10} is the shock area in units of 10 arcsec^2 and V_{100} in the wind velocity in units of 100 km s^{-1}. The total mass loss may be a good deal higher than this, since only a portion of the wind is effective in exciting the knots. However, it cannot exceed the above figure divided by the covering factor of the Herbig-Haro knot as seen from the central star: $\sim 3 \times 10^{-4}\ M_{\odot}$ yr^{-1}. This upper limit compares with the estimate of $3 \times 10^{-4}\ M_{\odot}$ yr^{-1} given by MBT on the basis of the OH observations.

Correcting for projection effects, we can use the shock velocity derived from the spectrophotometry and the observed radial velocity of each knot to estimate the systemic velocity. We find $V_{\mathrm{Hel}} = +26 \pm 22$ km s^{-1} from the N knot and $V_{\mathrm{Hel}} = +60 \pm 34$ km s^{-1} from the S knot, or, from both, $V_{\mathrm{Hel}} = +43 \pm 21$ km s^{-1} ($V_{\mathrm{LSR}} = 26 \pm 21$ km s^{-1}).

The picture that thus emerges of a high-velocity flow chaneled toward the poles of the nebula by a dense equatorial disk of ambient material, and in which the northern lobe is inclined toward the observer, is quite at variance with the model inferred by MBT. We must therefore ask whether the OH observations can be reconciled with this picture.

To answer this, we need to know what drives the high-velocity OH molecular flow in this object. According to the theory advanced by Calvet, Canto, and Rodriguez (1981), the force driving the molecular material in HH/T Tauri complexes is viscous coupling with a high-velocity wind stream. If this is the case in OH 0739−14, then the flows generated will move tangentially at the wind/circumstellar disk interface, and the entrainment of disk material means that this interface advances as the disk is slowly ablated away. Since we assume that the disk has its highest density in the equatorial plane, this process will generate a cusp in this plane. The geometry of the flow we are proposing will therefore look something like Figure 4. Working from the star outward, the flow zones are the unshocked stellar wind, the turbulent shock stellar wind interface, the molecular entrainment region in which the flow accelerates as it moves away from the central star, and, finally, a slow shock which is being driven into the circumstellar disk material. The OH maser emission arises in the entrainment region where densities are high enough and where the geometrical extension in the line of sight of material moving at a particular velocity is also high. As can be seen from Figure 4, we predict the peak of the maser emission at the largest nega-

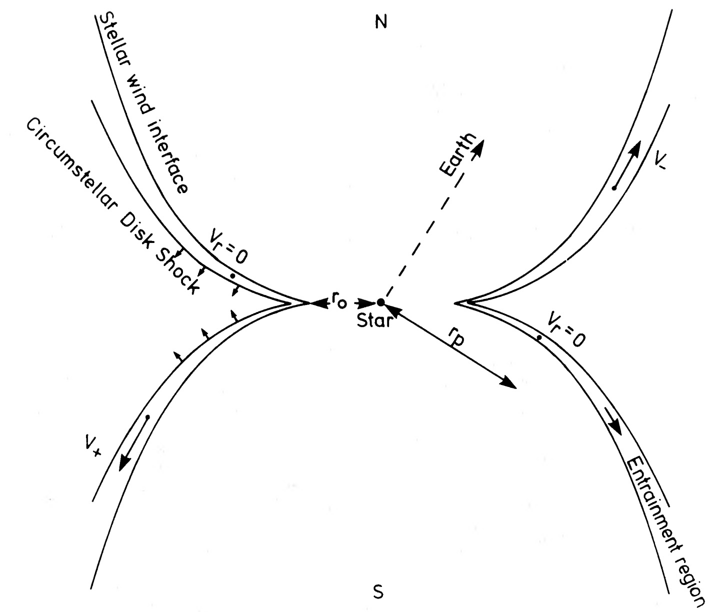

FIG. 4.—Schematic model of the structure of the inner disk region associated with the OH source. Maximum negative velocities occur in the region marked V_- associated with the N lobe, whereas positive velocities (V_+) are associated with the S lobe. The zero velocity emission will occur in a ring of radius r_p in the N-S direction and r_0 in the E-W direction. Molecular species not excited in the entrainment region should show a quite different dynamical structure.

tive velocities (V_-) seen to be associated with the northern lobe, and the corresponding maximum positive velocity (V_+) to be located in the southern lobe. This is what MBT observe. The zero radial velocity surface is also interesting. In this geometry it occurs in an approximately elliptical region extending out to r_0 in the plane of the sky and out to a projected distance r_p (see Fig. 4) at right angles to this. This is again what is seen by MBT with $r_p/r_0 \approx 1.25$ if the true systemic radial velocity is, in fact, about $+35$ km s^{-1} (V_{LSR}), corresponding to the center of the OH "plateau" emission. The "spike" seen by MBT at lower velocities is presumably associated with a greater degree of amplification occurring in the region of approaching gas (V_-) due to its favorable geometry, or, as suggested by Bowers and Morris (1984), as a result of amplified starlight. Thus, our model can explain the general features of the MBT observations, as well as conforming to what we think we know about the geometry and physics of bipolar ejection.

In closing, we would like to draw attention to the possible connection between OH 0739 − 14 and symbiotics, particularly of the "type II" class (Paczyński and Rudak 1980), which have often been proposed as protoplanetary nebulae. Although, of course, OH 0739 − 14 shows none of the emission-line spectrum which is part of the essential description of the symbiotic phenomenon (e.g., Allen 1984), nevertheless, the combination of red giant and blue star suggests a possible relationship. Furthermore, an increasing number of symbiotic stars have been inferred to have bipolar mass flow with velocities as high as 200 km s^{-1}. These include HM Sge, BF Cyg, V1016 Cyg, and R Aqr (Solf 1983, 1984; Ulrich *et al.* 1984). Finally, the typical masses estimated for symbiotic stars are 3–5 $M_\odot$ (Boyarchuk 1983). This is similar to the mass ($M > 3\ M_\odot$) inferred for OH 0739 − 14 on the basis of the overabundance of nitrogen in the associated Herbig-Haro objects. Symbiotic stars derive their energy and ultraviolet photons by accretion of the giant stars' stellar wind onto a compact companion, and this process of accretion may also produce dense equatorial disks and photoionized gas at intermediate ($\sim 10^6$ cm^{-3}) densities. We postulate that the same process is occurring in OH 0739 − 14 and that the energetic wind is derived from this process. However, the absence of nebular emission in the vicinity of the central stellar objects, seen either directly or else by reflection, is puzzling. If OH 0739 − 14 is indeed related to the symbiotics, then episodic rather than continuous outflow seems to be indicated. This is not at variance with what has been seen to occur in some symbiotics, in particular, HM Sge, which brightened by some 6 mag in 1975 (Dokuchaeva 1976). If we assume that gas ejected in such an event in OH 0739 − 14 has at present reached the position of the Herbig-Haro knots, then at an assumed velocity of ~ 200 km s^{-1} and for an assumed distance of ~ 2 kpc, this eruptive event occurred some 1000–2000 yr ago.

It is, at first sight, remarkable that bipolar ejections of HH objects can characterize such extremes of evolution as represented by T Tauri stars, on the one hand, and OH 0739 − 14, a red giant, on the other. However, we regard this as showing simply that similar geometry (a dense equatorial disk) and similar energetic phenomena (strong outflow from the central source) will produce similar dynamical effects (bipolar outflow, HH shocks). The fundamental difference between the two phases is that in the T Tauri stars the equatorial disk is the result of accretion, whereas in this red giant the disk results from earlier mass loss from the central star ejected at much lower velocities than the present-day wind velocity.

We wish to thank ATAC for their generous allocation of telescope time, and the director of the AAO for use of his facilities, particularly for the computing facilities at Siding Spring where the reduction of the observations was carried through.

We also thank Judy Cohen for sending us a print of her near-infrared photograph of OH 0739 − 14.

M. C. thanks the director of the National Optical Astronomy Observatories, Tucson, AZ, for travel support to Australia.

REFERENCES

Allen, D. A. 1984, *Proc. Astr. Soc. Australia*, **5**, 367.
Allen, D. A., Barton, J. R., Gillingham, P. R., and Phillips, B. A. 1980, *M.N.R.A.S.*, **190**, 531.
Baldwin, J. A., and Stone, R. P. S. 1984, *M.N.R.A.S.*, **206**, 241.
Becker, S. A., and Iben, I. J 1979, *Ap. J.*, **232**, 831.
Boksenberg, A. 1972, in *Proc. ESO/CERN Conf. Auxiliary Instrumentation for Large Telescopes*, ed. S. Lausten and A. Reitz (Hamburg: ESO), p. 295.
Bowers, P. F., and Morris, M. 1984, *Ap. J.*, **276**, 646.
Boyarchuk, A. A. 1982, in *The Nature of Symbiotic Stars*, ed. M. Friedjung and R. Violti (Dordrecht: Reidel), p. 11.
Calvet, N., Canto, J., and Rodriquez, L. F. 1981, *Bull. AAS.*, **13**, 784.
Canto, J. 1980, *Astr. Ap.*, **86**, 327.
Canto, J., and Rodriguez, L. F. 1981, *Ap. J.*, **239**, 982.
Cohen, M. 1981, *Pub. A.S.P.*, **93**, 288.
———. 1982, *Pub. A.S.P.*, **94**, 266.
Cohen, M., and Frogel, J. A. 1977, *Ap. J.*, **211**, 178.
Cohen, M., and Kuhi, L. V. 1980, *Pub. A.S.P.*, **92**, 736.
Cohen, M., and Schwartz, R. D. 1979, *Ap. J. (Letters)*, **233**, L77.
Dokuchaova, O. D. 1976, *Inf. Bull. Var. Stars*, No. 1189.
Dopita, M. A. 1978, *Ap. J. Suppl.*, **37**, 117.
Dopita, M. A., Binette, L., D'Odorico, S., and Benvenuti, P. 1984, *Ap. J.*, **276**, 653.
Dopita, M. A., Binette, L., and Schwartz, R. D. 1982, *Ap. J.*, **261**, 183.
Dopita, M. A., Schwartz, R. D., and Evans, I. 1982, *Ap. J. (Letters)*, **263**, L73.
Greig, W. E. 1971, *Astr. Ap.*, **10**, 161.
Isobe, S. 1975, *Ann. Tokyo Astr. Obs.*, **14**, 141.
Konigl, A. 1982, *Ap. J.*, **261**, 115.
Morris, M., and Bowers, P. F. 1980, *A.J.*, **85**, 724.
Morris, M., Bowers, P. F., and Turner, B. E. 1982, *Ap. J.*, **259**, 625.
Oke, J. B. 1974, *Ap. J. Suppl.*, **27**, 21.
Paczyński, B., and Rudak, B. 1980, *Astr. Ap.*, **82**, 349.
Peimbert, M. 1978, in *IAU Symposium 76, Planetary Nebulae*, ed. Y. Terzian (Dordrecht: Reidel), p. 215.
Raymond, J. C. 1979, *Ap. J. Suppl.*, **39**, 1.
Renzini, A. 1981*a*, in *Physical Processes in Red Giants*, ed. I. Iben, Jr., and A. Renzini (Dordrecht: Reidel), p. 431.
———. 1981*b*, in *Effects of Mass-Loss on Stellar Evolution*, ed. C. Chiosi and R. Stalio (Dordrecht: Reidel), p. 319.
Renzini, A., and Voli, M. 1981, *Astr. Ap.*, **94**, 175.
Schwartz, R. D. 1975, *Ap. J.*, **195**, 631.
Shull, J. M., and McKee, C. F. 1979, *Ap. J.*, **227**, 131.
Solf, J. 1983, *Ap. J. (Letters)*, **266**, L113.
———. 1984, *Astr. Ap.*, **139**, 296.
Stauffer, J. R. 1984, *Ap. J.*, **280**, 695.
Tielens, A. G. G. M., Werner, M., and Capps, R. 1985, in preparation.
Turner, B. E. 1971, *Ap. Letters*, **8**, 73.
Ulrich, H., Solf, J., and Herbig, G. H. 1984, in preparation.
Wood, P. R., and Cahn, J. H. 1977, *Ap. J.*, **211**, 499.
Wynn-Williams, C. G., Becklin, E. E., and Neugebauer, G. 1974, *Ap. J.*, **187**, 473.

MARTIN COHEN: Radio Astronomy Laboratory, University of California, Berkeley, and NASA/Ames Research Center, Moffett Field, CA 94035

MICHAEL A. DOPITA: Mount Stromlo and Siding Spring Observatories, Private Bag, Woden P.O., ACT 2606, Australia

RICHARD D. SCHWARTZ: University of Missouri, 8001 Natural Bridge Road, St. Louis, MO 63121

A. G. G. M. TIELENS: Space Science Laboratory, University of California, Berkeley, CA 94720